Application of the wave finite element method to reinforced concrete structures with damage

Evelyne El Masri, Neil Ferguson and Timothy Waters

Institute of Sound and Vibration Research, University of Southampton, Southampton SO17 1BJ, UK

E-mail: eem3g14@soton.ac.uk, nsf@isvr.soton.ac.uk, tpw@isvr.soton.ac.uk

Abstract. Vibration based methods are commonly deployed to detect structural damage using sensors placed remotely from potential damage sites. Whilst many such techniques are modal based there are advantages to adopting a wave approach, in which case it is essential to characterise wave propagation in the structure. The Wave Finite Element method (WFE) is an efficient approach to predicting the response of a composite waveguide using a conventional FE model of a just a short segment. The method has previously been applied to different structures such as laminated plates, thinwalled structures and fluid-filled pipes. In this paper, the WFE method is applied to a steel reinforced concrete beam. Dispersion curves and wave mode shapes are first presented from free wave solutions, and these are found to be insensitive to loss of thickness in a single reinforcing bar. A reinforced beam with localised damage is then considered by coupling an FE model of a short damaged segment into the WFE model of the undamaged beam. The fundamental bending, torsion and axial waves are unaffected by the damage but some higher order waves of the cross section are significantly reflected close to their cut-on frequencies. The potential of this approach for detecting corrosion and delamination in reinforced concrete beams will be investigated in future work.

1. Introduction

Most damage in reinforced concrete structures comprising steel bars is due to corrosion and delamination. Before any repair procedures can take place, this damage should be located and quantified. Because the repair and maintenance costs are considerable, an early detection of damage is needed. The majority of non-destructive techniques (NDT) require knowledge of the existence of the deterioration. Thus, vibration based methods have been developed as both global and local approaches to detect damage. These methods can be divided into modal and wave based methods. The modal methods require the modal characteristics, and the wave based methods require the wave characteristics of the structure. Therefore, the knowledge of wave characteristics is essential within a specified waveguide. Since the structure is a composite, analytical wave solutions do not apply. That is why a numerical approach is needed to determine the wave solution within the waveguide.

One approach to analyse a waveguide is the spectral finite element (SFE). However, this method requires new spectral mass and stiffness matrices for each scenario on a case-by-case basis[1]. Alternatively, the Wave Finite Element method (WFE) is adopted, where a small segment of the waveguide is modelled via FE. The displacements and forces at each DOF for different wave modes in the segment are then solved at each frequency step.

Mace and Duhamel presented the WFE method for simple homogeneous one dimensional waveguides. The efficiency and accuracy of this method was compared to the spectral FE method for the forced response. Wavenumbers and group velocity were presented and discussed for a beam, a simply supported plate strip and a viscoelastic laminate[2][3]. Mencik and Ichchou formulated and solved wave propagation in guided elastodynamic structures filled with acoustic fluid using WFE. Free and forced frequency response of the waveguide were presented, and comparisons between the proposed method and classical theories were formulated showing that this method is not limited to low frequencies[4]. Arrud *et al.* also compared the wave finite element and spectral element method. A simple Timoshenko Beam and Kirchhoff Levy plates were used for illustration[5]. In a later application, Waki *et al.* expressed free and forced vibrations of a tyre using the WFE formulation on a short circumferential segment, and results were compared to experiments[6]. In addition, they considered numerical issues concerning the wave and finite element method for free and forced vibrations of waveguides, and a robust procedure was proposed. There are many examples covering free wave propagation in an EulerBernoulli beam and a thin plate strip[7]. Renno and Mace formulated a rectangular segment as a waveguide via WFE. Then, the forced response to a convected harmonic pressure (CHP) was formulated, where a comparison was presented between FE and WFE predictions of a frequency response function for a cantilever-laminated beam[1]. Furthermore, they calculated the forced response of two-dimensional homogeneous media via WFE. Numerical examples covered isotropic, orthotropic and laminated plates[8].

Zhou *et al.* compared wave propagation results between the semi-analytical finite element (SAFE) method and WFE for a steel pipe. Efficiency and accuracy of both methods were examined[9]. Renno and Mace calculated the reflection and transmission coefficients of joints using a hybrid finite element/wave and finite element approach, where the joint is modelled via FE and a small portion of the waveguide is expressed via WFE. The two waveguides are coupled in order to get the reflection and transmission coefficients of the joint. Forced response examples were presented for two rods connected at a point mass, an L-frame configuration, and lap-jointed laminated beams with a slot[10].

One of the major advantages of the WFE method is that the solutions as displacement and forces at each DOF can be used to couple damaged and undamaged waveguides to predict the reflection and transmission coefficients due to a defect. For instance, Ichchou et al. formulated the WFE method to obtain the displacement and force solutions for a rectangular cross section waveguides. The diffusion matrix prediction model (DMM) was used to couple damaged and undamaged waveguides, where higher modes show sensitivity to damage modelled as a notch within the section[11]. In addition, Zhou and Ichchou expressed wave excitation and scattering using the eigensolutions from WFE of coupled structures comprising damaged and undamaged plates[12]. Later, they used the WFE method to obtain the wave characteristics of a curved beam. Mode conversion, reflection and transmission coefficients were used to localize the damaged portions[13].

Subsequently, Kharrat proposed the identification and sizing of defects in pipelines by the wave finite element method using torsional guided waves. Reflections from cracks are expressed as a methodology to identify damage sizing. WFE was adapted to predict the wave characteristics of hollow cylinders, and good agreement was found with respect to full finite element simulation[14]. In addition, Kharrat *et al.* used WFE to construct a numerical database of reflection coefficients by varying the dimensions of damage in pipelines. Torsional guided waves were also proposed for pipeline inspection[15].

In this paper, WFE is applied to a reinforced deep concrete beam section where the displacement and force solutions are found. Dispersion curves and mode shapes are plotted for the least attenuated waves. Then, reflection coefficients associated with the presence of a damaged section are computed to inspect and comment upon their sensitivity to an introduced

defect representing the corrosion of a steel rebar.

2. WFE formulation

The WFE concept relies on the notion of predicting the wave characteristics of a structure through analysing the wave propagation within a short section of the waveguide, and by expressing the continuity of displacements and equilibrium of forces at the boundaries between successive segments, an eigenvalue problem is posed in terms of a transfer function across the section. By solving this problem at each specified frequency, the eigenvalues obtained,that are related to the wavenumbers of the waveguide, relate the variables to the right and left side of the section, and the eigenvectors are associated with the displacement and forces at this section.

The length of the Δ section should not be too small with respect to the shortest wavelength to avoid round off errors, nor too large to reduce discretization errors[7]. The dynamic stiffness matrix is then developed using the mass and stiffness matrices. Commercial FE packages are used to model the waveguide section and to extract the required matrices. In this paper, ANSYS is used to model the reinforced waveguide section. After extracting the mass and stiffness matrices, the dynamic stiffness matrix is processed to formulate the transfer matrix, and then the eigenvalue/eigenvector problem is solved to express the wavenumbers and eigenvectors at each frequency of interest. The key expressions and relationships are given briefly below.

The dynamic stiffness matrix of a finite waveguide relating the element nodal displacements and forces is given at frequency ω by

$$\mathbf{D} = \mathbf{K} - \omega^2 \mathbf{M} \tag{1}$$

where $\mathbf{K}$ and $\mathbf{M}$ are the $N \times N$ stiffness and mass matrices of the waveguide section, where N is the total number of DOFs . The transfer function matrix must ensure the continuity of displacements $\boldsymbol{q}$ and equilibrium of forces $\boldsymbol{f}$ between the boundaries of two consecutive elements[2]. L and R are designated for the left and right sides as in Figure 1. The dynamic stiffness matrix is partitioned accordingly.

$$\begin{bmatrix} \boldsymbol{D_{LL}} & \boldsymbol{D_{LR}} \\ \boldsymbol{D_{RL}} & \boldsymbol{D_{RR}} \end{bmatrix} \begin{bmatrix} \boldsymbol{q_L} \\ \boldsymbol{q_R} \end{bmatrix} = \begin{bmatrix} \boldsymbol{f_L} \\ \boldsymbol{f_R} \end{bmatrix} \tag{2}$$

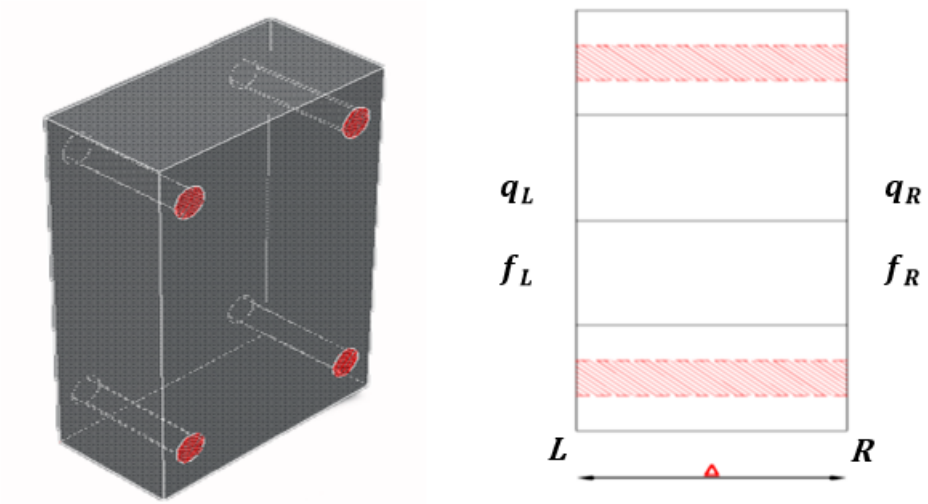

Figure 1. WFE waveguide section of a reinforced concrete beam of length Δ

The periodic conditions for the displacements and the equilibrium condition at the junction of the two elements are $\boldsymbol{q_R}=\lambda \boldsymbol{q_L}$; $\boldsymbol{f_R}=-\lambda \boldsymbol{f_L}$ where the propagation constant $\lambda = e^{-ik\Delta}$ relates the right and left displacements and forces, and k is the wavenumber.

Equation(2) can be rearranged and written as

$$\lambda \begin{Bmatrix} \boldsymbol{q_L} \\ \boldsymbol{f_L} \end{Bmatrix} = \mathbf{T} \begin{Bmatrix} \boldsymbol{q_L} \\ \boldsymbol{f_L} \end{Bmatrix} \tag{3}$$

with $\mathbf{T}$ as the transfer matrix,

$$\mathbf{T} = \begin{bmatrix} -\boldsymbol{D_{LR}^{-1}} \boldsymbol{D_{LL}} & \boldsymbol{D_{LR}^{-1}} \\ -\boldsymbol{D_{RL}} + \boldsymbol{D_{RR}} \boldsymbol{D_{LR}^{-1}} \boldsymbol{D_{LL}} & -\boldsymbol{D_{RR}} \boldsymbol{D_{LR}^{-1}} \end{bmatrix} \tag{4}$$

The transfer matrix eigenvalue problem is solved at each frequency step, where the wavenumbers k are related to the eigenvalues. The positive-going waves are characterized by $\left|\lambda_j^+\right| < 1$ and the negative going waves by $\left|\lambda_j^+\right| > 1$. However, for $\left|\lambda_j^+\right| = 1$, the associated waves are considered positive-going if they fulfil the condition $Re\left\{\boldsymbol{f_L^H} \dot{\boldsymbol{q}}_{\boldsymbol{L}}\right\} = Re\left\{i\omega \boldsymbol{f_L^H} \boldsymbol{q_L}\right\} < 0$. Furthermore, the wave modes associated with the eigenvectors for solutions of Equation(3) are grouped into positive and negative-going waves

$$\Phi^+ = [\Phi_1^+ \cdots \Phi_N^+]; \Phi^- = [\Phi_1^- \cdots \Phi_N^-]; \Phi = [\Phi^+ \quad \Phi^-] \tag{5}$$

where each wavemode is divided into displacement $\boldsymbol{q}$ and force $\boldsymbol{f}$ sub-vectors, i.e.

$$\Phi_j = \begin{Bmatrix} \Phi_{\boldsymbol{q}} \\ \Phi_{\boldsymbol{f}} \end{Bmatrix}_j \tag{6}$$

The rapidly decaying wavemodes are removed due to their negligible contribution to the far field response, and to reduce ill-conditioning[7]. Thus, only m pairs of positive and negative going waves are retained based on a user-defined criterion at each frequency step.

3. Reinforced concrete modelling in ANSYS

In order to apply the WFE method to a reinforced concrete beam, a section needs to be modelled in ANSYS in order to extract the associated mass and stiffness matrices. Concrete is modelled using the SOLID65 element in ANSYS which is a 3D solid element. It has three DOFs, which are translations in the X, Y and Z directions, and it is defined by eight nodes. Reinforcement rebars are modelled via the 3D discrete element REINF264 embedded in the SOLID65 element. The nodal locations, degrees of freedom and connectivity of the REINF264 element are identical to those of the base element which is the SOLID65[16]. The location of the rebar is defined as an offset distance from the edges of the base element selected, as shown in Figure 2. The undamaged reinforced concrete section is modelled using 16 SOLID65 elements, with the dimensions and properties shown in Figure 3 and Table 1. The total number of DOFs N is 150 for this model.

The damaged reinforced concrete section is modelled in the same way as for the undamaged section except that the area of the damaged reinforced rebar at the right bottom corner is reduced to represent a loss of thickness due to corrosion. In this model, the corroded rebar is taken to have a diameter equivalent to a 44 percent reduction compared to the intact one. The mass and stiffness matrices were extracted using ANSYS software for both the damaged and undamaged sections, and then post-processed using WFE. There are 150 different wavenumbers in accordance with number of DOFs, but most of them have a significant imaginary part corresponding to highly attenuated waves, and therefore need to be eliminated. In this model, only the wave modes associated with $|Im\,(k\Delta)| \leq 0.3$ are retained at each frequency step. This corresponds to an attenuation of 10 dB along the element length in the propagating direction.

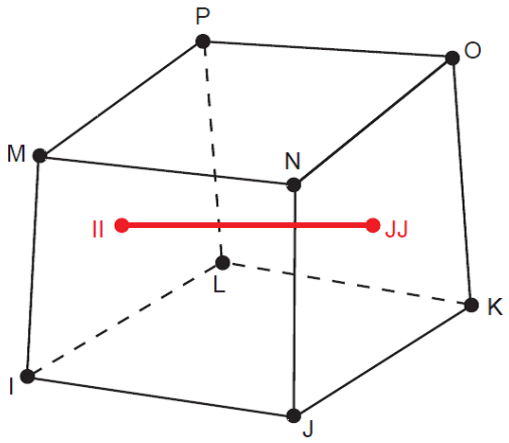

Figure 2. SOLID65 element (nodes I-J-K-L-M-N-O-P) representing the concrete with embedded (nodes II-JJ) REINF264 representing the discrete reinforcement

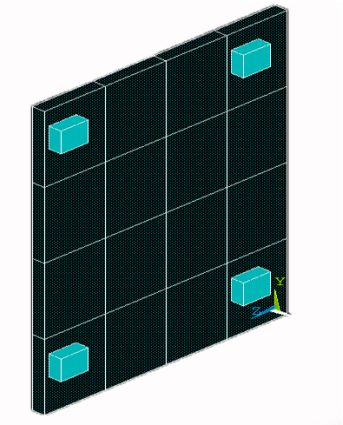

Figure 3. Modelling of undamaged reinforced concrete section in ANSYS using 16 SOLI65 and 4 REINF264 elements at corners

Properties	**Concrete**		**Steel**	
Dimensions	Length of element Δ (m)	0.01	Rebar area (m^2)	0.00051
	Length in y-direction (m)	0.2	-	-
	Length in z-direction (m)	0.3	-	-
Material	Young Modulus (Pa)	25×10^9	Young Modulus (Pa)	200×10^9
	Poisson ratio ν	0.18	Poisson ratio ν	0.3
	Density ρ (kg/m^3)	2400	Density ρ (kg/m^3)	7850

Table 1. Dimensions and material properties of concrete and steel materials

4. Dispersion relations and wave mode shapes

The wave modes are evaluated within the frequency range of 1 to 15 kHz with a frequency step of 50 Hz. The dispersion curves relating to the least attenuated waves are plotted for both the damaged and undamaged waveguides. Figure 4 presents the dispersion curves for those modes that can propagate over the whole frequency band. Only the real part of the wavenumbers is plotted, since with no damping in the model the imaginary part is zero. Mode 1 is associated with axial motion, mode 2 with torsional around the x-axis, and modes 3 and 4 with bending in the vertical and transverse directions respectively. Figure 5 presents the dispersion curves of the waves that are evanescent at low frequency. However, Figure 6 presents the dispersion curves of the complex modes at low frequency for both waveguides, where the wavenumber is complex below the cut-on frequency. Above cut-on, the wavenumber becomes purely real. In all cases, only a slight change is observed between the wavenumbers associated with the damaged and undamaged waveguides. This due to the fact that the majority of the structural stiffness is governed by the concrete rather by the reinforcement rebars.

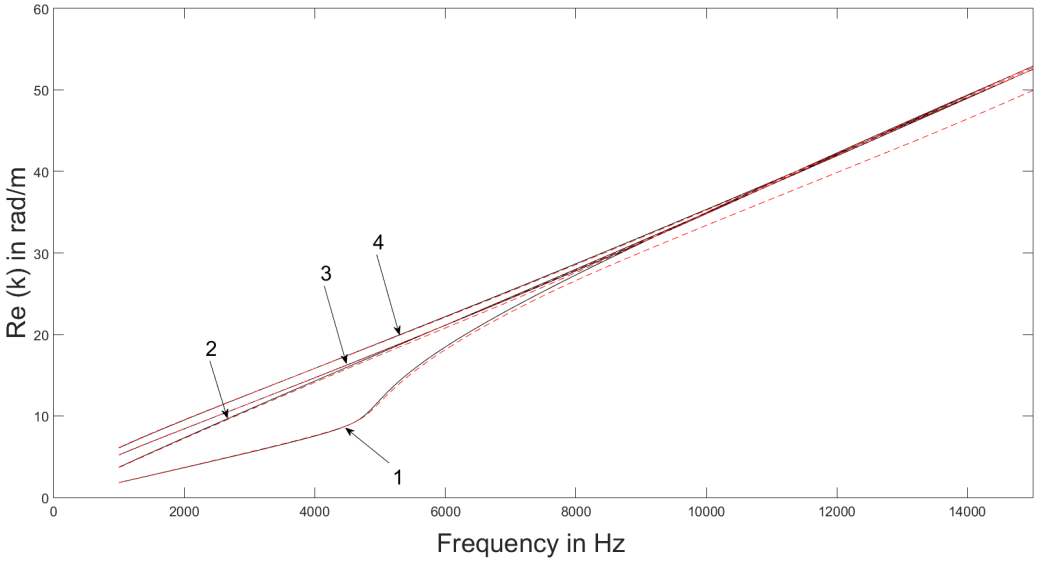

Figure 4. Dispersion curves for the real part of the wavenumbers for propagating wave modes over the whole frequency band: Undamaged section (—), Damaged section (- - -)

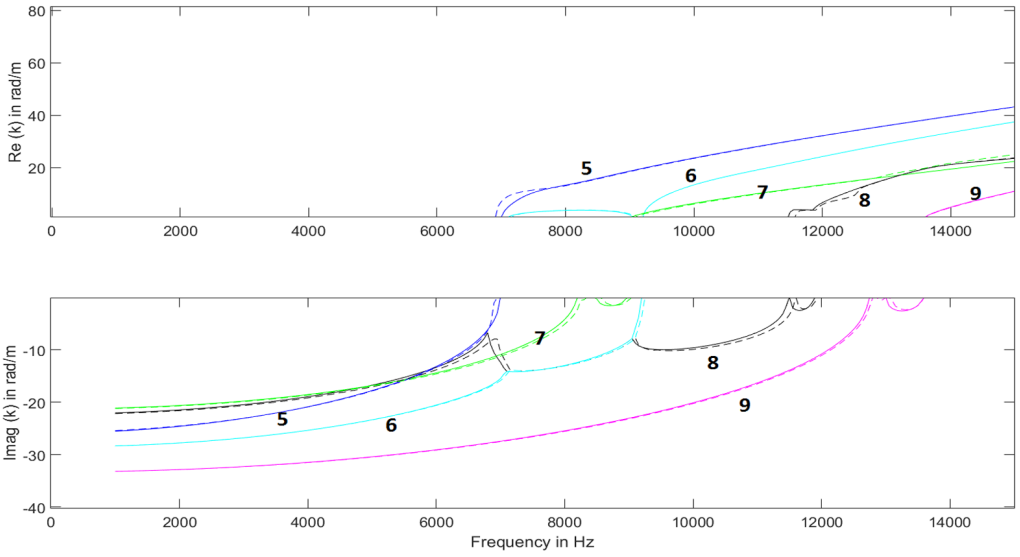

Figure 5. Dispersion curves for the real and imaginary parts of the wavenumbers for evanescent wave modes at low frequency: Undamaged section (—), Damaged section (- - -)

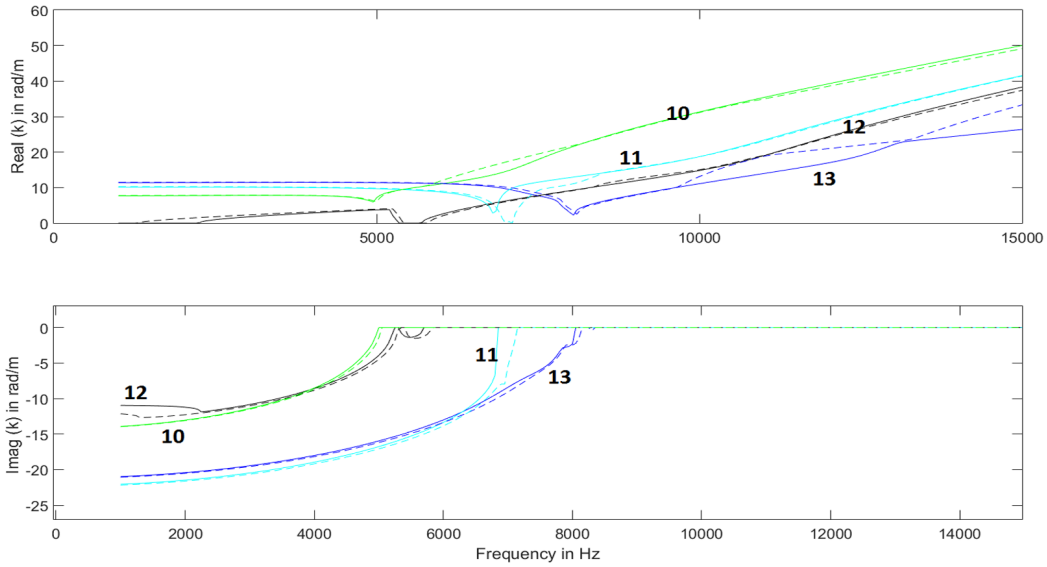

Figure 6. Dispersion curves for the real and imaginary parts of the wavenumbers for complex wave modes at low frequency: Undamaged section (—), Damaged section (- - -)

After solving the eigenvalue/eigenvector problem, one can plot the wave mode shapes by extracting the nodal displacements from Equation (6). Figure 7 presents the wave mode shapes of the undamaged waveguide at low frequency for modes 1 to 4. The contour lines illustrate the nodal displacement in the x-axis on the cross section of the waveguide for each of these corresponding modes.

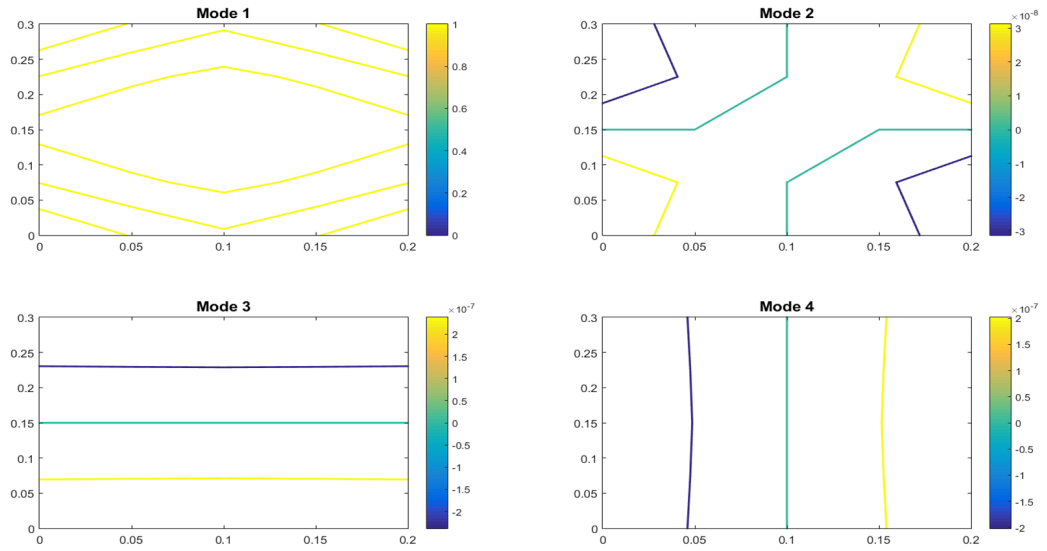

Figure 7. Wave mode shapes at low frequency for propagating waves in the undamaged waveguide (x-axis direction)

5. Scattering properties of the damaged section

Damage or discontinuities in structures influence the scattering properties for incident waves, potentially being of use for damage inspection. One can model the damaged and undamaged waveguides as two semi-infinite beams, and couple the waves at the interface of the junction. This model is denoted here as the WFE-WFE approach. However, where considering the case where one reinforcement corrosion is introduced and the length of the damaged member plays a significant role, coupling of a finite damage section to undamaged waveguides is a more appropriate model. In this case, a WFE-FE-WFE coupling approach van be used[10] and it is adopted here.

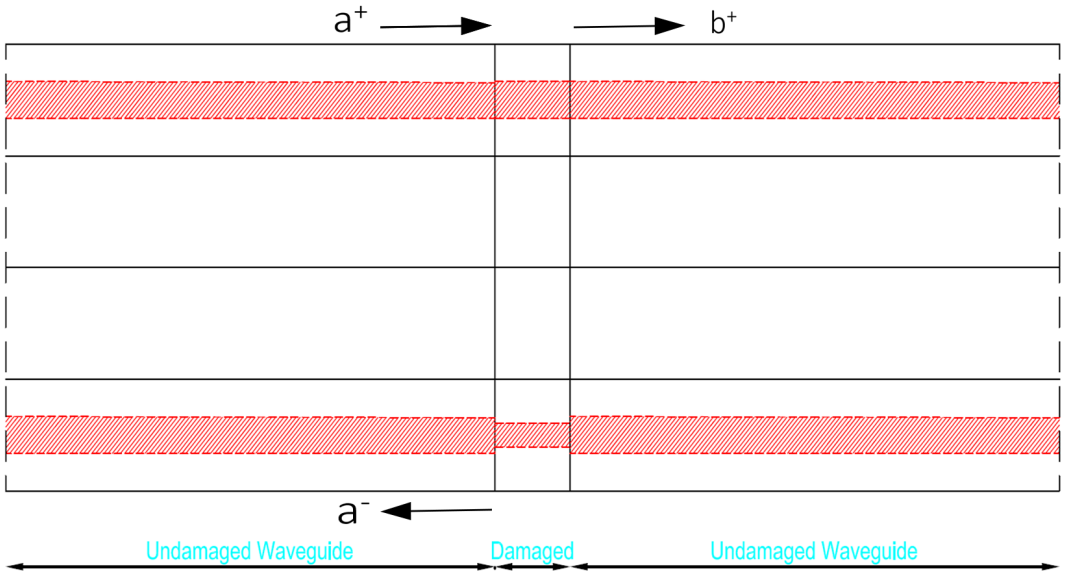

Figure 8. The interface between wave finite element model of the undamaged waveguides connected to a finite element model of the damaged section

In this model, the undamaged waveguide is connected to a damaged section. Then, the undamaged waveguide is modelled using the WFE method as explained earlier. However, the damaged section is modelled via FE of a finite length Δ_i= 0.01m. The effect of the length of the damaged section and wave propagation in each waveguide will be investigated in a future work. Both interfaces are compatible since they have the same nodal meshes and DOFs as shown in Figure 8. The interface nodes are expressed by i, and non-interface ones are denoted by n. For this model, only the reflection coefficients present in the scattering matrix of the wave propagating from the undamaged section to the damaged section are of interest. Transmission coefficients and wave mode conversion will be considered in future work.

The damaged section is characterized by the relationship between displacements and forces as

$$\begin{bmatrix} \tilde{\boldsymbol{D}}_{ii} & \tilde{\boldsymbol{D}}_{in} \\ \tilde{\boldsymbol{D}}_{ni} & \tilde{\boldsymbol{D}}_{nn} \end{bmatrix} \begin{bmatrix} \mathbf{Q}_i \\ \mathbf{Q}_n \end{bmatrix} = \begin{bmatrix} \mathbf{F}_i \\ \mathbf{F}_n \end{bmatrix} \tag{7}$$

with $\mathbf{Q}$ the vector of DOFs and $\mathbf{F}$ as the vector of internal nodal forces. $\tilde{\boldsymbol{D}}$ is the dynamic stiffness matrix of the damaged section. Setting $\mathbf{F}_n = 0$ since no external forces are applied at the non-interface nodes, $\tilde{\boldsymbol{D}}$ can be dynamically condensed into $\boldsymbol{D}_{ii}$, that only contains the interface nodes, by

$$\mathbf{D}_{ii} = \tilde{\boldsymbol{D}}_{ii} - \tilde{\boldsymbol{D}}_{in}\tilde{\boldsymbol{D}}_{nn}^{-1}\tilde{\boldsymbol{D}}_{ni} \tag{8}$$

Equation 7 becomes

$$\mathbf{D}_{ii}\mathbf{Q}_i = \mathbf{F}_i \tag{9}$$

By implementing the continuity and force equilibrium conditions, the nodal DOFs and forces at the interfaces are equal to those of the undamaged waveguides on each side, i.e

$$\mathbf{Q}_i = \boldsymbol{q} \quad ; \quad \mathbf{F}_i = \boldsymbol{f} \tag{10}$$

The amplitude of the incident waves on the interface denoted by $\mathbf{a}^+$ give rise to reflected waves of amplitudes $\mathbf{a}^- = \mathbf{r}\mathbf{a}^+$ and transmitted waves of amplitudes $\mathbf{b}^+ = \mathbf{t}\mathbf{a}^+$, with $\mathbf{r}$ and $\mathbf{t}$ as the reflection and transmission coefficients of the damaged section. In addition, vectors $\boldsymbol{q}$ and $\boldsymbol{f}$ can be written as sum of the positive and negative going waves

$$\boldsymbol{q} = \Phi_{\boldsymbol{q}}^+\mathbf{a}^+ + \Phi_{\boldsymbol{q}}^-\mathbf{a}^- \quad ; \quad \boldsymbol{f} = \Phi_{\boldsymbol{f}}^+\mathbf{a}^+ + \Phi_{\boldsymbol{f}}^-\mathbf{a}^- \tag{11}$$

Then, Equation 9 becomes

$$[\Phi_{\boldsymbol{f}}^+ - \mathbf{D}_{ii}\Phi_{\boldsymbol{q}}^+]\mathbf{a}^+ + [\Phi_{\boldsymbol{f}}^- - \mathbf{D}_{ii}\Phi_{\boldsymbol{q}}^-]\mathbf{a}^- = \mathbf{0} \tag{12}$$

where $\Phi_{\boldsymbol{q}}^+$, $\Phi_{\boldsymbol{f}}^+$, $\Phi_{\boldsymbol{q}}^-$, and $\Phi_{\boldsymbol{f}}^-$ are block matrices. Then, the scattering matrix is given by

$$\boldsymbol{S} = -[\mathbf{D}_{ii}\Phi_{\boldsymbol{q}}^- - \Phi_{\boldsymbol{f}}^-]^{-1}[-\Phi_{\boldsymbol{f}}^+ + \mathbf{D}_{ii}\Phi_{\boldsymbol{q}}^+] \tag{13}$$

The scattering matrix $\boldsymbol{S}$ is a block matrix where the diagonal matrices comprise the reflection coefficients, and the off-diagonal matrices contain the transmission coefficients. In this model, reflection coefficients of the damaged section are of interest.

6. Numerical results

The undamaged section is modelled similarly to the previous part in WFE. The damaged part is modelled in ANSYS of dimensions and properties similar to the one modelled in WFE previously of length equal to 0.01 m. Consequently, $\boldsymbol{S}$ is calculated at each frequency step of 50 Hz and significant reflection coefficients are plotted for wave modes within the frequency range of 1 to 15 kHz. Since modes 1 to 4, which propagate at all frequencies, have small reflection coefficients within this frequency range, they are not plotted. However, evanescent modes 5 to 9 and complex modes 10 to 13 provide higher reflection coefficients associated with their cut-on frequencies as shown in Figure 9. Wave mode shapes for the real part of the displacement at these cut-on frequencies are presented in Figure 10. Consequently, this type of damage in one of the reinforced rebars is potentially detectable by high order wave modes since they present higher reflection coefficients when they cut-on.

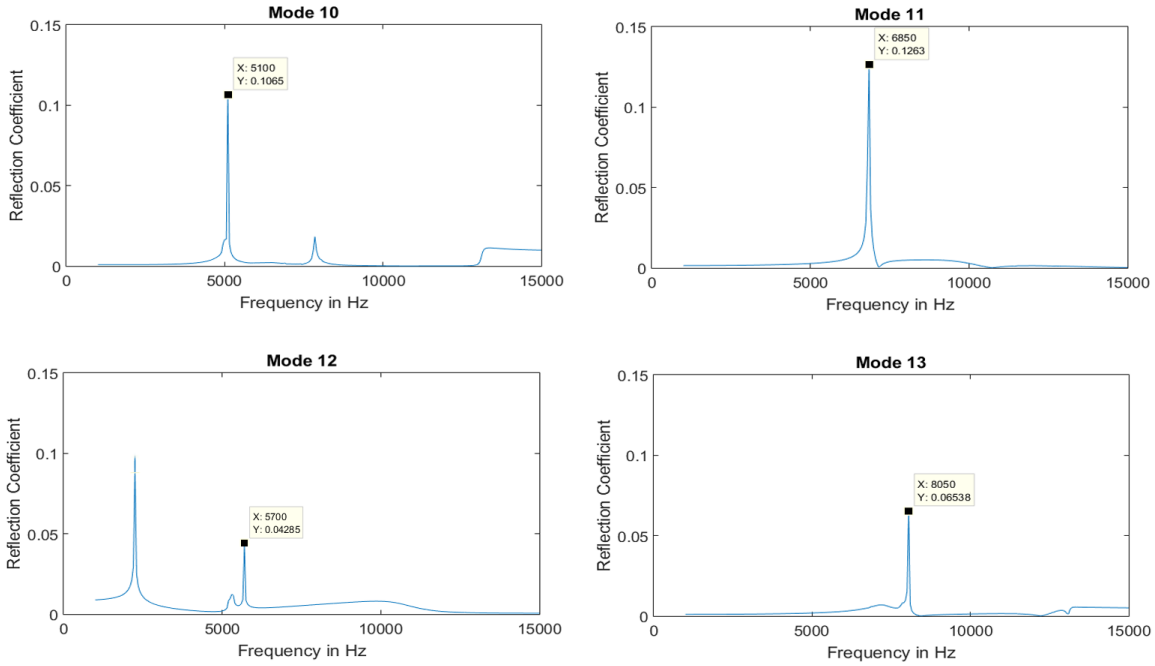

Figure 9. Magnitude of the reflection coefficients for wave modes with respect to frequency

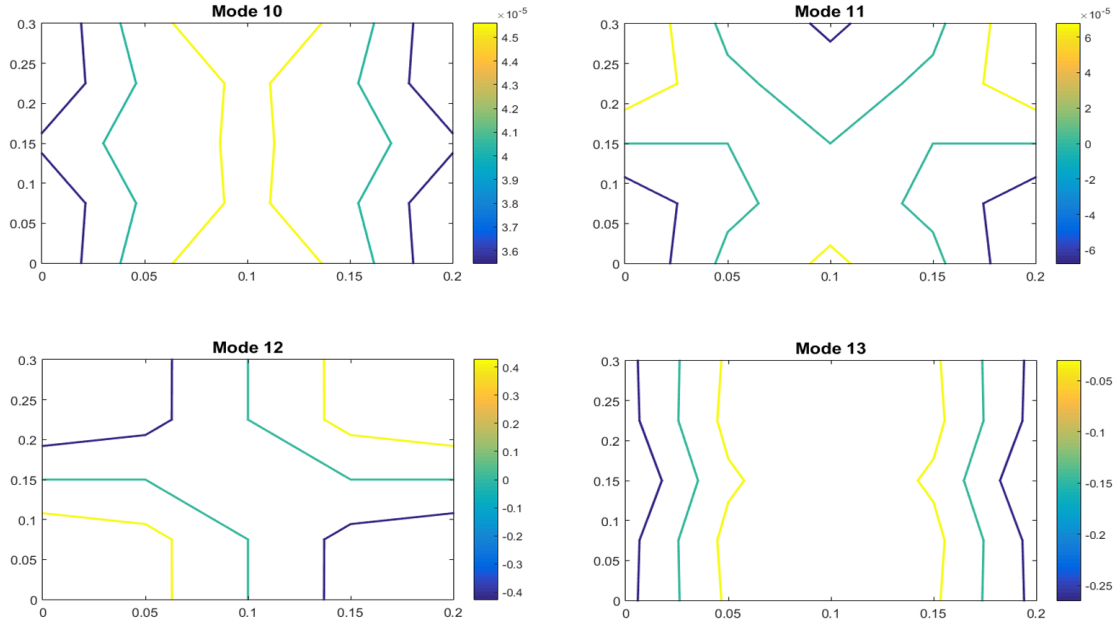

Figure 10. Magnitude of reflection coefficients of wave modes with respect to frequency

7. Discussion

Modes 10 to 13, which are cross section modes, have shown sensitivity to damage occuring at one of the corners of the deep RC beam. This sensitivity is highlighted by their reflection coefficients due to damage at the mode cut-on frequencies. This effect can be shown by the shift in the

cut-on frequencies between the damaged and undamaged waveguides in Figure 6, which causes the sudden increase in the reflection coefficients at this particular frequency. Table 2 shows these shifts for modes 10 to 13.

Mode 12 is described as torsional around the y-axis. However, modes 10, 11 and 13 are shear dominant. This sensitivity should be inspected according to damage variabilities: the percentage of diameter reduction of the damaged rebar, the number of rebars damaged within the cross section of the concrete and the length of the damage. These variabilities will be highlighted in future work and considered for practical use in experimental investigations.

Mode Number	**10**	**11**	**12**	**13**
Cut–on frequency of undamaged section in Hz	5000	6850	5700	8050
Cut–on frequency of damaged section in Hz	5050	7150	5850	8150

Table 2. Higher order mode cut-on frequencies for the damaged and undamaged waveguides

8. Conclusions

In order to define wave characteristics in reinforced concrete, the WFE was applied to a reinforced deep concrete beam section for both damaged and undamaged waveguides. The damaged section is modelled as a reduction of the cross sectional area of the rebar representing the extent of the damage. Dispersion curves and mode shapes are plotted for the least attenuated waves. Then, coupling between damaged and undamaged waveguides was developed via the hybrid FE/WFE method. The scattering matrix was formulated, and the reflection coefficients associated with the damaged section were computed. Higher order modes have shown higher sensitivity to potential damage of the reinforcement rebar at their cut-on frequencies and could be considered for further study and practical application.

References

[1] Renno J M and Mace B R 2010 *Journal of Sound and Vibration* **329** 5474–5488
[2] Duhamel D, Mace B R and Brennan M J 2006 *Journal of Sound and Vibration* **294** 205–220
[3] Mace B R, Duhamel D, Brennan M J and Hinke L 2005 *Journal of the Acoustical Society of America* **117(5)** 2835–2843
[4] Mencik J M and Ichchou M N 2007 *International Journal of Solids and Structures* **44** 2148–2167
[5] Arruda J R F, Ahmida K M, Ichchou M N and Mencik J M 2007 *19th International Congress of Mechanical Engineering, Braslia, DF*
[6] Waki Y, Mace B R and Brennan M J 2009 *Journal of Sound and Vibration* **323** 737–756
[7] Waki Y, Mace B R and Brennan M J 2009 *Journal of Sound and Vibration* **327** 92–108
[8] Renno J M and Mace B R 2011 *Journal of Sound and Vibration* **330** 5913–5927
[9] Zhou W J, Ichchou M N and Bareille O 2011 *Structural Control and Health Monitoring* **18** 737–751
[10] Renno J M and Mace B R 2013 *Journal of Sound and Vibration* **332** 2149–2164
[11] Ichchou M N, Mencik J M and Zhou W 2009 *Computer Methods in Applied Mechanics and Engineering* **198** 1311–1326
[12] Zhou W and Ichchou M 2010 *Structural Health Monitoring* **10** 335–349
[13] Zhou W J and Ichchou M N 2010 *Computer Methods in Applied Mechanics and Engineering* **199** 2099–2109
[14] Kharrat M, Bareille O, Ichchou M N and Zhou W 2011 *COMPDYN 2011, ECCOMAS Thematic Conference on Computational Methods in Structural Dynamics and Earthquake Engineering*
[15] Kharrat M, Ichchou M N, Bareille O and Zhou W 2014 *International Journal of Applied Mechanics* **06** 1450035
[16] ANSYS 2013 *ANSYS Mechanical APDL Element Reference*